# DEEP-WATER DOLOMITES FROM THE PROTEROZOIC PENGANGA GROUP IN THE PRANHITA-GODAVARI VALLEY, ANDHRA PRADESH, INDIA

JOYDIP MUKHOPADHYAY[1], S.K. CHANDA[2], M. FUKUOKA[3], AND ASRU K. CHAUDHURI[4]*

[1] *Department of Geology, Durgapur Govt. College, Durgapur, West Bengal 713214, India*

[2] *Department of Geological Sciences, Jadavpur University, Calcutta 700032, India*

[3] *Hiroshima University, Hiroshima, Japan*

[4] *Geological Studies Unit, Indian Statistical Institute, 203 Barrackpore Trunk Road, Calcutta 700035, India*

ABSTRACT: **The middle to upper Proterozoic Penganga Group of the Pranhita-Godavari valley, South India, contains a thick slope-to-basin limestone-shale succession. The limestone, the Chanda Limestone, is well bedded and micritic with several interbeds of slope-related autoclastic debris-flow lime-clast conglomerates in its lower part. The limestone near its base encloses a 30 m thick interval of rhythmically alternating centimeter- to decimeter-thick beds of limestone and dolomitic limestone. The autoclasts of debris-flow conglomerates within the dolomite-bearing sequence shows similar rhythmic repetition of dolomite and limestone. Dolomite crystals range in size from micrite to 225 μm and have planar-s to idiotopic-p fabrics. A dolomitic bed contains 40–45% dolomite. The dolomite content commonly decreases from the base to the top of a bed with decline in frequency and size of coarse dolomite rhombs. The dolomite is nonstoichiometric ($Ca_{0.54-0.56}Mg_{0.46-0.44}CO_3$) and has cloudy core with inclusions of micritic calcite and dolomite. The $\delta^{13}C_{PDB}$ values of limestone and dolomite vary between +2.0‰ to +3.4‰ and +3.8‰ to +4.3‰, respectively. The $\delta^{18}O_{PDB}$ values of limestone and dolomite range from −6.0‰ to −7.6‰ and +0.4‰ to −8.7‰, respectively. Stratigraphic, petrographic, and geochemical studies suggest dolomitization in normal marine pore water during shallow burial diagenesis. Rhythmicity is attributed to recurrent episodes of dolomitization with $Mg^{2+}$ derived mainly from dissolution of precursor high-magnesium calcite. A mass-balance calculation suggests that 9 mole % $MgCO_3$ in the precursor would provide sufficient $Mg^{2+}$. Normal grading of dolomite rhombs suggests that upward movement of Mg-enriched pore water dolomitized a thin interval of limestone wherever the Mg content reached the threshold for dolomitization.**

## INTRODUCTION

Several dolomitization models explain coastal to shallow marine dolomites that require some "special" conditions to overcome a plethora of kinetic factors inhibiting direct precipitation of dolomite from normal marine water (Badiozamani 1973; Folk and Land 1975; Zenger et al. 1980; Machel and Mountjoy 1986; Hardie 1987). None of these models treats deep-marine dolomites directly, although dolomite is now recognized as a common component in modern deep-marine sediments and averages about 1% of post-Jurassic deep-sea sediments (Lumsden 1985, 1988). Many workers have proposed the idea of precipitation of penecontemporaneous dolomite from normal sea water or pore water in equilibrium with sea water (Saller 1984; Mullins et al. 1985; Mullins et al. 1988; Mitchell et al. 1987; Lumsden 1988) from subtidal to deep-marine environments. Documentation of pre-Tertiary deep-marine dolomitization, however, is yet very rare (Coniglio and James 1988).

Here we report a stratified, centimeter- to decimeter-scale rhythmic succession of limestone and dolomitic limestone from the deep-marine middle to upper Proterozoic Chanda Limestone of the Penganga Group in the intracratonic Pranhita-Godavari valley basin of Andhra Pradesh, India (Fig. 1). The deep-water carbonate-shale succession is unmetamorphosed and shows no evidence of fresh-water diagenesis. The dolomite not only is a rare record of Proterozoic dolomitization but is also unique because it records rhythmic dolomitization from a deep-marine setting. Sarkar (1991) and Sarkar et al. (1993) invoked a hydrothermal origin for these dolomites through fault-controlled circulation of deep basinal brines. Here we propose an alternative shallow-burial origin in the presence of marine pore water, on the basis of an integrated study of stratigraphy, petrography, and stable isotopes.

## GEOLOGICAL SETTING

The Penganga Group is part of the middle to upper Proterozoic Godavari Supergroup (Chaudhuri and Chanda 1991) and is situated in the northwestern margin of the Pranhita-Godavari valley basin (Fig. 1). The Penganga Group around Adilabad (Andhra Pradesh) has been divided into three formations (Fig. 2; Chaudhuri et al. 1989): the Pranhita Sandstone, the Chanda Limestone, and the Sat Nala Shale, in ascending order. All or parts of the Penganga Group have been structurally repeated in down-dip sections by strike-parallel *en echelon* thrust sheets.

The Pranhita Sandstone is a thin, cross-bedded, shallow-water sandstone and is overlain by the deep-marine Chanda Limestone. The Chanda Limestone is micritic, with massive to laterally persistent plane-parallel beds defined by varying proportions of carbonate and shale. The lower and middle parts of this limestone include several horizons of channelized or sheet-like beds of autoclastic, lime-clast conglomerates of debris-flow origin (Chaudhuri et al. 1989; Bose and Sarkar 1991). Shallow-marine carbonates as well as siliciclastic detritus coarser than silt are completely absent. The basal part and the uppermost part of the limestone is brown and the middle part is black. The transition from basal brown to black takes place through pink and steel-gray intervals (Fig. 3A), and that from the black to the upper brown takes place through a steel-gray interval. The Chanda Limestone has been interpreted as a slope-to-basin deposit (Chaudhuri et al. 1989).

## METHODOLOGY

Thin sections stained with Alizarin red-S and potassium ferricyanide (cf. Friedman 1959) were studied to distinguish dolomite from calcite. Fifteen samples of pure dolomite from dolomite beds and eight samples of limestone were obtained for isotope analysis by drilling out crystals. Samples were analyzed for stable carbon and oxygen isotopes at the University of Texas at Austin. For limestones, samples were dissolved in anhydrous $H_3PO_4$ at 25°C, whereas dolomite samples were dissolved at 25°C and 50°C. Analyses were carried out in a Nuclide mass spectrometer. The $\delta^{18}O_{PDB}$ values for dolomite were corrected at 25°C (a dolomite sample reacted with $H_3PO_4$ at 50°C is depleted in $\delta^{18}O$ by 1.22‰ relative to samples reacted with $H_3PO_4$ at 25°C; see Gao and Land 1991). Analytical reproducibility for $\delta^{18}O_{PDB}$ and $\delta^{13}C_{PDB}$ values based upon replicates of NBS 19 and 20 standard and unknowns is better than ± 0.1‰. Trace-element analyses for assessing Sr content were carried out from powdered pellets of four samples in a sequential X-ray spectrometer, PW 1480, at the Hokkaido University, Japan. Elemental analyses of dolomites and calcites were obtained from the Department of Geology, Kyushu University, Japan, using a EPMA JEOL/JXA-8600 model. Carbon-coated surfaces

* Correspondence address.

JOURNAL OF SEDIMENTARY RESEARCH, VOL. 66, NO. 1, JANUARY, 1996, P. 223–230
 1073-130X/96/066-223/$03.00

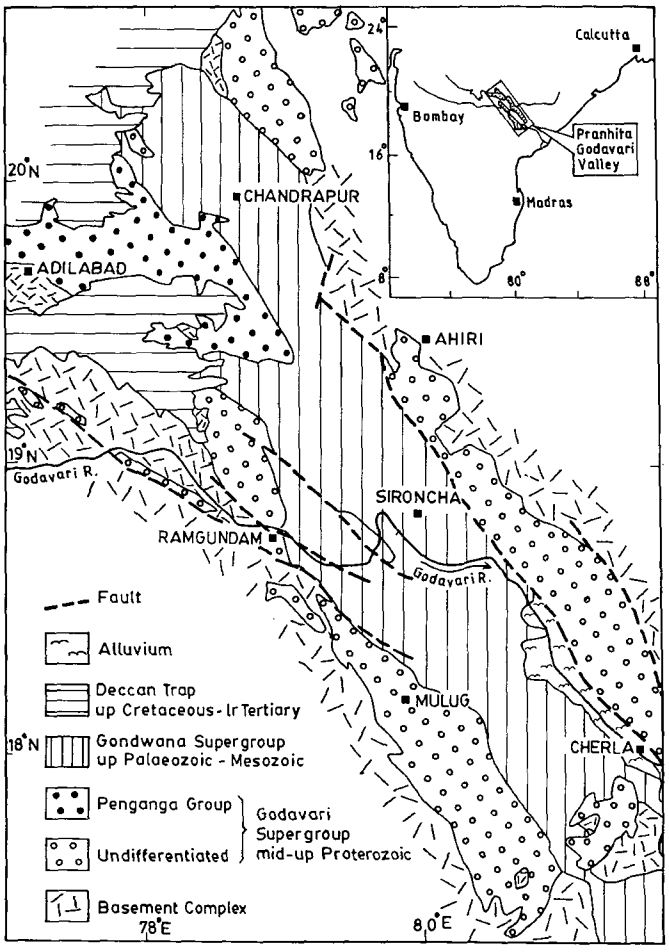


FIG. 1.—Generalized map of the Pranhita-Godavari Valley (after Chaudhuri and Chanda 1991).

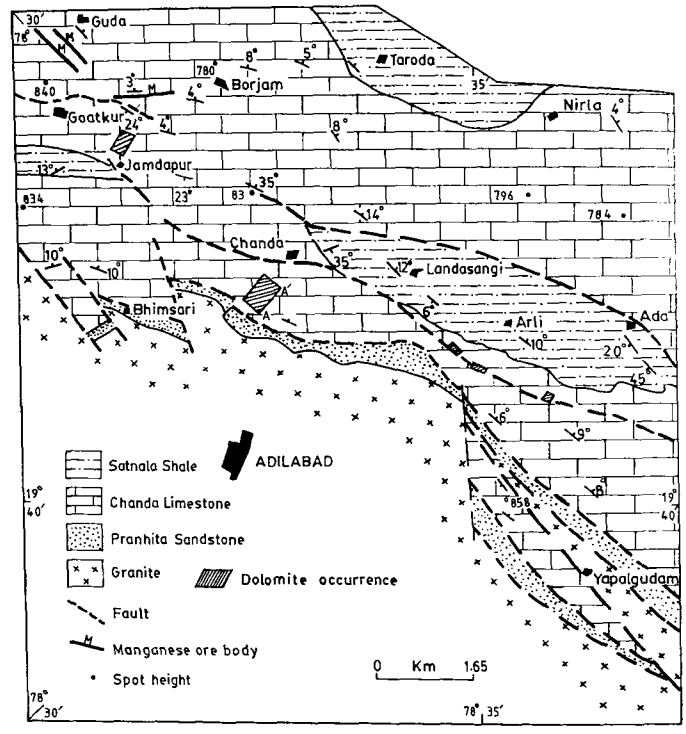


FIG. 2.—Geologic map of the area around Adilabad, Andhra Pradesh, India. Dolomite-bearing sequence is marked by hatched areas. Section AA' along Mathadi Vagu.

were analyzed with accelerating voltage of 10 kV, specimen current of 0.020 μA, and 1–2 μm electron beam diameter. For standards, natural MgO, $Fe_2O_3$, MnO, $CaSiO_3$, $BaSO_4$, and $Al_2O_3$ were used. The matrix correction method of Bence and Albee (1968) was adopted.

## DISTRIBUTION OF DOLOMITE

Dolomite is present mainly in the lower brown and pink intervals of the Chanda Limestone. These are best exposed in a succession 30 m thick in the basal thrust package, 3 km northwest of Adilabad, along the Mathadi Vagu section. Other exposures are north of Jamdapur and Yapalgudam (Fig. 2) within thrust packages that are down-dip sections at the equivalent stratigraphic level.

In the Mathadi Vagu section (Fig. 3A) dolomite is present in the upper 8 m of brown limestone and lower 22 m of the overlying pink limestone. The dolomite-bearing succession includes one 3.5 m thick channelized body of lime-clast conglomerate. Dolomite is present as subparallel beds 1.5–15 cm (average 2 cm) thick alternating with thicker limestone beds (average 4 cm) (Figs. 3B, 4). A similar alternation of limestone and dolomitic limestone is also found in the clasts of the lime-clast conglomerates in the dolomite-bearing interval. Each dolomitic bed can be traced laterally for a few meters to tens of meters until it pinches out or is abruptly truncated by stylolites at lateral margins (Fig. 4). The dolomitic beds are commonly gradational to superjacent limestone. Their contacts with subjacent limestone beds are usually sharp, though gradational contacts are also found in places. Stylolites, common at or close to dolomite-limestone contacts, cause millimeter-scale discordance of the contacts. There are relict patches of limestone locally in the dolomitic beds.

## PETROGRAPHY

The limestones are micrite and show neither any effect of recrystallization beyond micrite stage nor any imprint of fresh-water diagenesis (e.g., James and Choquette 1984). A few crystals of micritic dolomite are scattered in the micritic limestones. Dolomitic beds, on the other hand, are composed of varying proportions of calcitic micrite and dolomite. Dolomite crystals vary in size between micrite to coarse (10–225 μm), subidiotopic to idiotopic rhombs. Commonly, the rhombs contain sparse inclusions of both micritic calcite and dolomite (Fig. 5) identical to the groundmass. Several rhombs show inclusions of optically disoriented smaller dolomite rhombs (Fig. 6).

On the basis of frequency of coarser dolomite crystals three fabric types can be distinguished in the dolomitic beds (Fig. 7).

Type A fabric: interlocking, coarse dolomite crystals with local intercrystalline patches of micrite, dominantly of calcite with dispersed micritic dolomite (identified by staining). The coarser rhombs (10–200 μm; Fig. 7A) form almost 95% of the total components. The interlocking crystals show planar intergranular boundaries typical of idiotopic-s (Sibley 1982) or planar-s fabric (Fig. 5; Sibley and Gregg 1987). This fabric is common in the lower to middle parts of dolomitized layers.

Type B fabric: coarse dolomite rhombs dispersed in a micritic groundmass, giving rise to idiotopic porphyrotopic texture (Figs. 7B, 8; Sibley 1982). The coarser rhombs (10–225 μm) form 30% of the total components. The groundmass consists of micrites of both dolomite and calcite, and is similar to interstitial patches in the Type A fabric.

Type C fabric: idiotopic porphyrotopic fabric with 10–120 μm dolomite crystals. The coarse crystals float in a groundmass of dolomitic and calcitic micrite (Figs. 7C, 9) and form 10% of the total constituents. This fabric

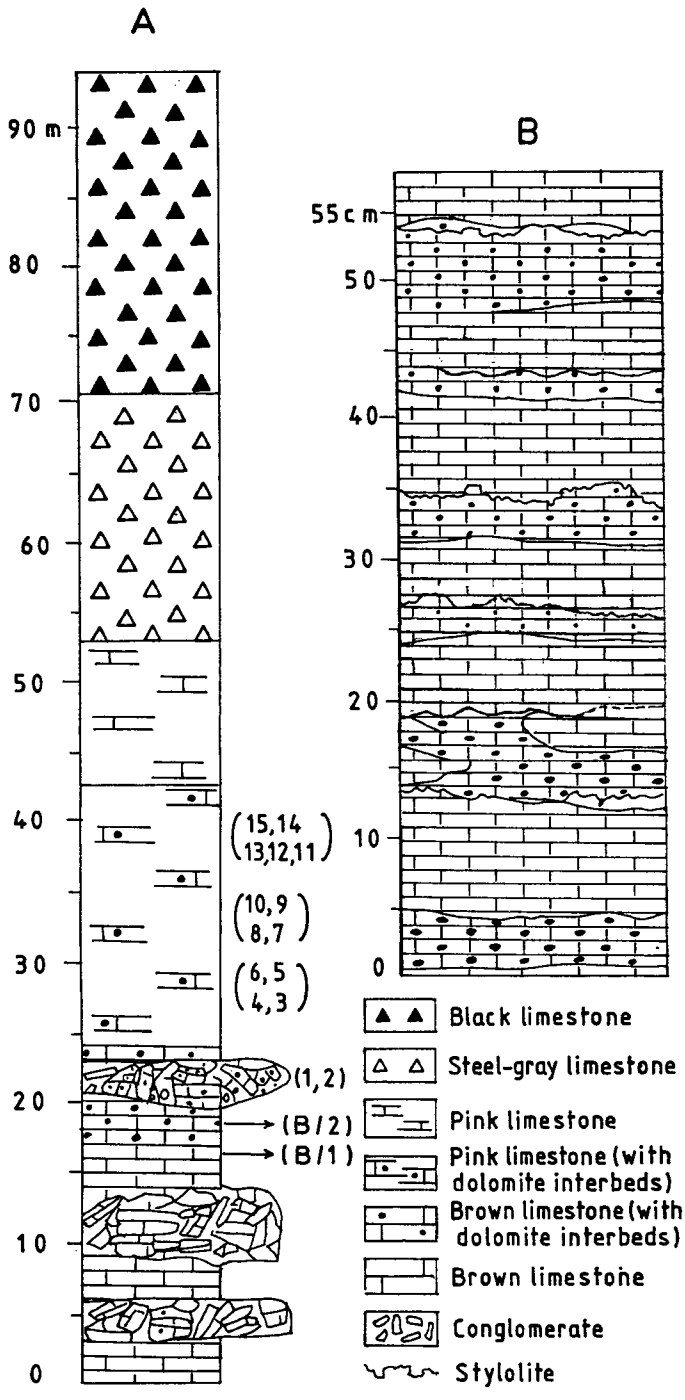


FIG. 3.—**A)** Litholog of Chanda Limestone at Mathadi Vagu Section, AA' in Figure 2, near Chanda village causeway on National Highway 7. Note sample positions collected for isotope studies. **B)** Detail log of dolomite-bearing sequence at the same location.

differs from Type B in its smaller crystal size and lower abundance of coarse rhombs.

Within a dolomitic bed, Type A fabric commonly is present at the base, overlying the subjacent limestone with sharp contact and passes upward through Type B into Type C fabric (Fig. 10) and then into the overlying limestone bed. Commonly, a dolomite bed shows a gradual decrease in dolomite content from Type A to Type C fabric. This change is reflected

FIG. 4.—Dolomite-limestone alternation. Lighter layers are dolomite. Note bedding-parallel dolomitization, and unreplaced limestone patches (darker areas) within dolomite beds. Note late-stage veins (arrow) at high angle to the bedding.

mainly in the decline in size and frequency of coarser dolomite rhombs. Fabric boundaries are commonly gradational, but Type A fabric locally shows sharp boundaries against Type B fabric (Fig. 11). In one instance, Type C fabric sharply overlies Type A with a stylolite at the contact (Fig. 12). Rarely, inverse grading of crystal size of rhombs was found at the base of a dolomite bed, where Type A fabric is preceded by Type B fabric. Stylolites, though not ubiquitous, are common at limestone-dolomite contacts. Petrographic studies reveal that stylolites either conform to the crystal boundaries or bind idiotopes (Fig. 13).

Commonly, a dolomitic bed shows a gradual decrease in dolomite content from Type A to Type C fabric. This change is reflected mainly in the decline in size and frequency of coarser dolomite rhombs. Modal analysis of stained thin sections suggests that a dolomitic bed consisting of all three fabrics contains 30–35% coarse dolomite rhombs (> 10 μm) and 65–70% micrite. Visual estimates suggest that micrite-size dolomites form 15–20% of the micritic groundmass. Overall a dolomitic bed contains 40–45% dolomite.

FIG. 5.—Photomicrograph of Type A fabric. Note intergranular micrite patches with dispersed micritic dolomites (stained thin section; darker patches are calcites) and similar relict micrite within rhombs. Note subidiotopic dolomite crystals with planar intergranular boundaries showing planar-s fabric. Scale bar 75 μm.

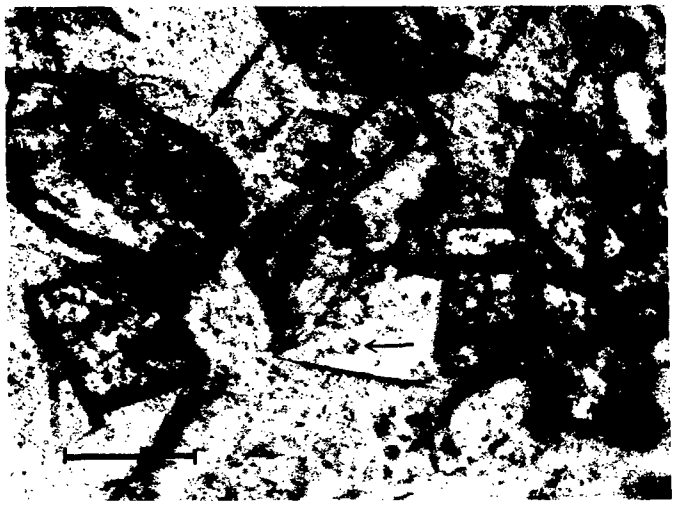

FIG. 6.—Photomicrograph showing optically discontinuous small rhomb (arrow) within coarse rhombs. Scale bar 100 μm.

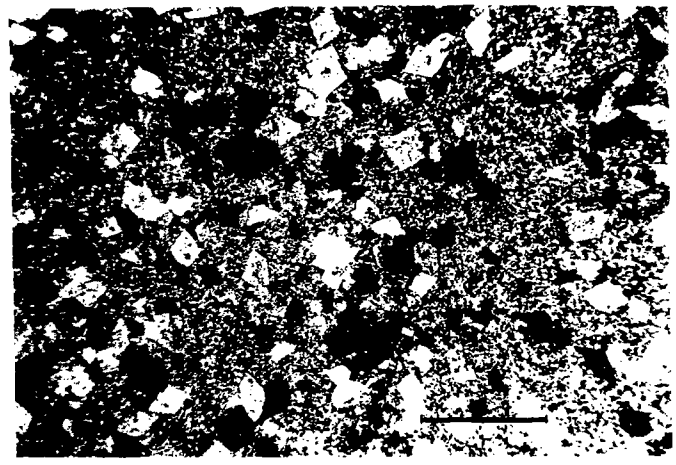

FIG. 8.—Photomicrograph of Type B fabric (crossed polars). Note coarse idiotopic to subidiotopic dolomite rhombs dispersed within micritic groundmass defining an idiotopic-p fabric. Scale bar 360 μm.

## GEOCHEMISTRY

Electron probe microanalysis of dolomite and calcite crystals shows that dolomite is nonferroan and nonstoichiometric ($Ca_{0.56-0.54}Mg_{0.44-0.46}CO_3$) whereas calcite contains about 1 mole % $MgCO_3$.

Isotope analyses (Table 1; see Figure 3A for relative position in dolomite-bearing interval) show that $\delta^{13}C_{PDB}$ values of limestone from the dolomite-bearing succession range from +2.0‰ to +3.4‰ and those of dolomite range from +3.8‰ to +4.3‰. $\delta^{18}O_{PDB}$ of dolomites range from +0.4‰ to −8.7‰ and those of limestones range from −6.0‰ to −7.6‰ (Fig. 14). Ten out of fifteen dolomites yield a near zero to low negative range (+0.4‰ to −4.8‰), while five others show lower values (−7.1‰ to −8.7‰). Four samples, B/2, 12, 14, and 15 (Table 1), from the dolomite-bearing succession show a Sr content of 82, 92, 100, and 103 ppm, respectively. Samples from other stratigraphic levels show a relatively higher range of values from 180 ppm to 354 ppm in siliceous gray limestone, steel-gray limestone, and black limestone (Table 1).

## ORIGIN

Integration of stratigraphic, petrographic, and geochemical data leads us to believe that dolomitization of Chanda Limestone is associated with shallow-burial marine diagenesis. Rhythmic alternation of dolomite and limestone in the clasts of the debris-flow conglomerate strongly suggests that the clasts were derived from penecontemporaneously dolomitized beds. Interlocking grain boundaries, abundant planar compromise boundaries, relict micritic calcite, and optically disoriented small dolomite crystals within coarse dolomite rhombs suggest progressive crystal growth through replacement of micritic groundmass. The planar-s fabric in Type A suggests

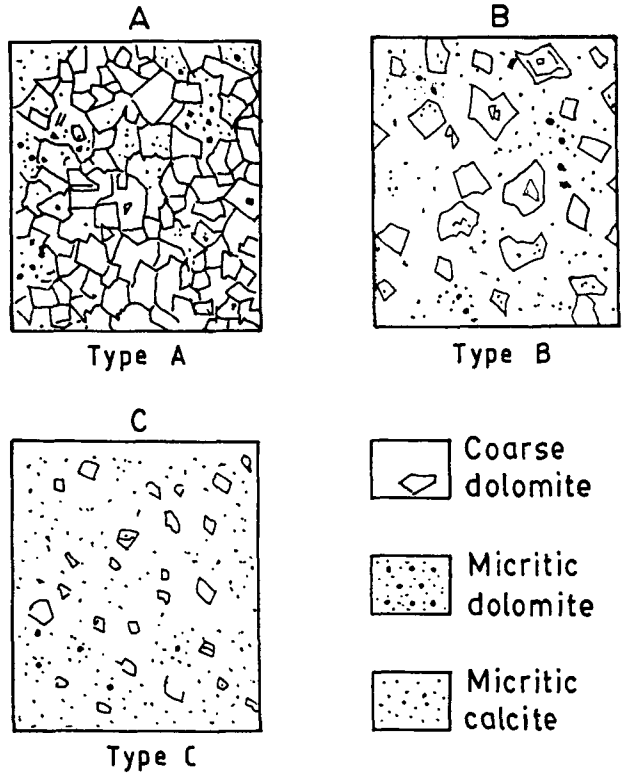


FIG. 7.—Schematic drawing of **A)** Type A, **B)** Type B, and **C)** Type C dolomite fabrics.

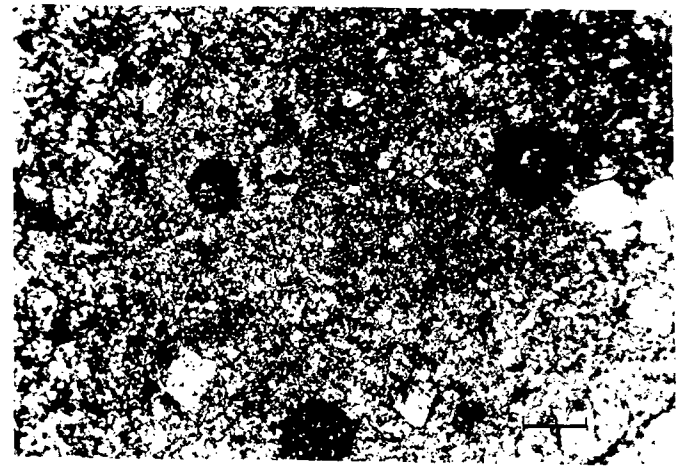

FIG. 9.—Photomicrograph showing Type C fabric (stained thin section); note rare coarser dolomite crystals dispersed within groundmass of micritic calcites (dark) and dolomites (white). Scale bar 100 μm.

FIG. 10.—Photomicrograph showing transition from Type B to Type C fabric; note decline in frequency of coarse dolomite crystals from B to C fabric. Scale bar 200 μm.

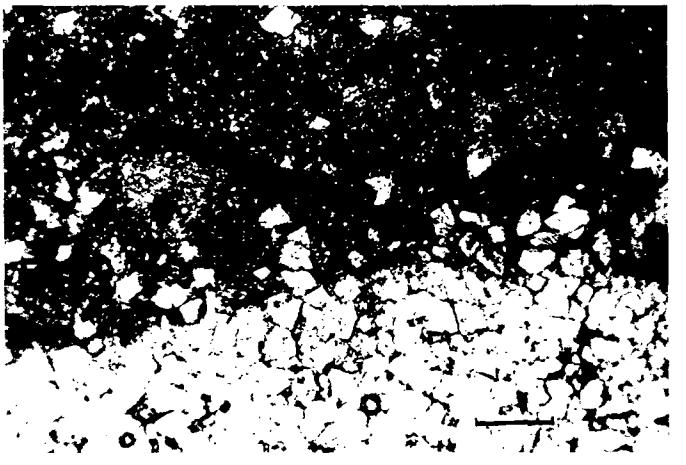

FIG. 12.—Photomicrograph showing sharp boundary between Type A and Type C fabric with a stylolite in between. Scale bar 240 μm.

slow grain growth under continuous flux of dolomitizing fluid at low temperature (Sibley and Gregg 1987).

The low positive range of $\delta^{13}C_{PDB}$ values of both dolomite and limestone suggests normal marine water (Hudson 1977; Anderson and Arthur 1983; Mullins et al. 1988). Low positive to low negative $\delta^{18}O_{PDB}$ (+0.4‰ to -4.85‰) of 10 out of 15 dolomite samples suggest precipitation from "marine-like" pore fluid during shallow subsurface diagenesis. Five samples with lower $\delta^{18}O_{PDB}$ values (−7.1‰ to −8.7‰) values record progressive dolomitization during shallow burial (Choquette and James 1990; Coniglio and Jones 1992; Smith and Dorobek 1993). The nonstoichiometric composition of these Proterozoic dolomites also suggests a syndepositional to early diagenetic, non-evaporitic, marine pore water origin (Lumsden and Chimahusky 1980) and low water/rock ratio (Sperber et al. 1984).

The notion of early diagenetic dolomitization by normal marine diagenesis is in contrast with the model of hydrothermal dolomitization through fault-controlled basinal, evaporitic brine (Sarkar 1991; Sarkar et al. 1993). We have not recognized any fault- or fracture-related dolomite. Bedding-parallel, repetitive dolomitization without any signature of bedding-discordant vein dolomite precludes fault-related hydrothermal process (Migaszewsky 1991; Mountjoy and Halim-Dhirajda 1991; Dix 1993). Subsurface brine is likely to give rise to massive dolomite instead of rhythmic alternation of limestone and dolomitic limestone (Gao and Land 1991; Gao et al. 1992). Moreover, dominantly low negative $\delta^{18}O_{PDB}$ values do not support a hydrothermal origin (Gregg 1988; Migaszewsky 1991).

Lumsden (1988) suggested precipitation of micritic dolomite (averaging 6 μm) from normal marine pore water in Recent deep-sea sediments. Mullins et al. (1988) also reported authigenic dolomites (10–20 μm) from pore water as cold as 1.8–9.8°C from the Neogene Florida–Bahamas platform, and Tucker (1983) reported early diagenetic dolomitization in the Proterozoic Beck Spring Formation. However, direct precipitation of abundant dolomite from normal marine pore water is inhibited by a number of factors. The main problem is the source of Mg. Enrichment of the pore water in Mg through dissolution of high-Mg calcite may be a plausible alternative (Cander et al. 1988), leading to partial dolomitization (Sperber et al. 1984). Factors such as high Mg/Ca ratio (Schwab 1978) and higher temperature (Perry and Ahmad 1983) of the sea water during the Precambrian could have facilitated precipitation of high-Mg calcite and aragonite (see also Grotzinger 1989). Many Precambrian limestones are believed to have pristine high-Mg calcite mineralogy (e.g., Tucker 1984). Excellent fabric preservation in many Precambrian dolomites strongly favors a dominant high-Mg calcite in the precursor sediment (Tucker 1982, 1983; Tucker and Wright 1990, p. 420). On the other hand, an aragonitic precursor of dol-

FIG. 11.—Photomicrograph showing sharp boundary between Type A and Type B fabrics. Scale bar 170 μm.

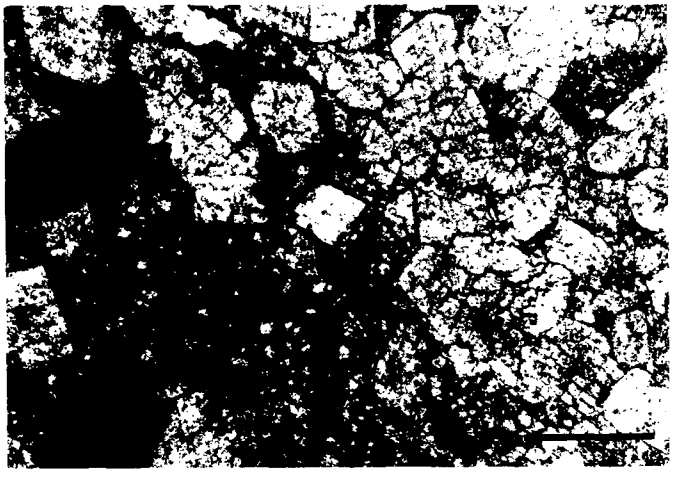

FIG. 13.—Photomicrograph showing relationship between stylolite and dolomite. X = pre-stylolitic dolomite. Scale bar 400 μm.

TABLE 1.—*$\delta^{13}C_{PDB}$ and $\delta^{18}O_{PDB}$ values and Sr content in dolomite and limestone*

| Sample No. | Description of Samples* | Limestones $\delta^{13}C_{PDB}$ (‰) | Limestones $\delta^{18}O_{PDB}$ (‰) | Dolomites $\delta^{13}C_{PDB}$ (‰) | Dolomites $\delta^{18}O_{PDB}$ (‰) | Sr (ppm) |
|---|---|---|---|---|---|---|
| B/1 | Brown limestone at the base of dolomite-bearing sequence | +3.4 | −7.6 | | | |
| B/2 | Dolomite | | | +4.0 | +0.4 | 82 |
| 1 | Dolomite-bearing clast of conglomerate | | | +4.1 | −8.7 | |
| 2 | Same as above | | | +4.0 | −8.6 | |
| 3 | Dolomite | | | +4.1 | −1.1 | |
| 4 | Limestone-dolomite couplet | +2.1 | −7.0 | +3.8 | −4.8 | |
| 5 | Dolomite | | | +4.4 | −3.7 | |
| 6 | Dolomite | | | +4.2 | −3.0 | |
| 7 | Limestone-dolomite couplet | +2.0 | −7.1 | +4.2 | −1.2 | |
| 8 | Dolomite | | | +4.3 | −0.2 | |
| 9 | Dolomite | | | +4.0 | −2.9 | |
| 10 | Dolomite | | | +4.1 | −0.9 | |
| 11 | Limestone-dolomite couplet | +2.0 | −6.0 | +4.2 | −2.5 | |
| 12 | Limestone | +2.2 | −6.8 | | | 92 |
| 13 | Dolomite | | | +4.1 | −7.3 | |
| 14 | Dolomite | | | +4.1 | −7.4 | 100 |
| 15 | Limestone-dolomite couplet | +2.3 | −6.7 | +4.3 | −7.1 | 103 |
| 16 | Siliceous gray** Limestone | +1.6 | −8.1 | | | 180 |
| 17 | Steel-gray Limestone** | +0.6 | −6.3 | | | 354 |
| 107 | Steel-gray Limestone** | | | | | 338 |
| 108 | Black limestone** | | | | | 337 |

* Sample position for samples from dolomite-bearing sequence shown in Fig. 3A. ** Samples 16, 17, 107, and 108 are from different stratigraphic levels.

omites would favor a higher Sr content, in the range of 300 to > 500 ppm (e.g., Fairchild and Spiro 1987; Mullins et al. 1988) or even higher, several thousand ppm (Tucker 1992). The Sr content of dolomites may of course be reduced during recrystallization or transformation from a nonstoichiometric to a stoichiometric state (Land 1980, 1985). The persistent low Sr content of the dolomites and the interbedded limestones without any evidence of recrystallization beyond the micrite stage would support a high-Mg calcite precursor rather than aragonite (Veizer et al. 1978). Repetitive development of limestone-dolomite couplets and successions of fabric types from A through B to C within the dolomitic limestone bed can be explained by diagenetic alteration of an Mg-calcite precursor. Incongruent dissolution of Mg-calcite under shallow burial would enrich the pore fluid with respect to $Mg^{2+}$. Net upward movement of pore fluid, thus enriched in $Mg^{2+}$, would initiate nucleation of dolomite as the $Mg^{2+}$ concentration in the pore fluid reaches the threshold value. Progressive dolomitization would gradually diminish the strength of the pore fluid upwards, leading to successive development of Type A to C fabrics (Fig. 15, Stages 1, 2, and 3). Continued sedimentation would move the sediment-water interface upward away from the zone of dolomite growth (Fig. 15, Stage 3). With time, dissolution of high-Mg calcite again leads to supersaturation to the point of formation of a new layer of dolomite (Fig. 15, Stages 3, 4, and 5). Spacing of the dolomitic and limestone beds is thus a result of sedimentation rate; that is, rate of upward migration of sediment-water interface, rate of Mg-calcite dissolution, and rate of Mg depletion by growth of dolomite. A similar diagenetic mechanism has been proposed by Jenkyns (1974), Dean et al. (1977), and Eder (1982) to explain cyclicity between nodule-rich and clay-rich layers in pelagic carbonate successions. Furthermore, cyclic variation in the rate of sedimentation (i.e., rate of burial) is inherent to many carbonate slope environments (Dean et al. 1977; Einsele 1982). Such variation affecting the extent of alteration of the precursor high-Mg calcite in the sedimentary column may also facilitate cyclic development of dolomite with shallow subsurface diagenesis (see also Scoffin 1987, p. 143).

A cyclic variation in the mineralogy as reported from many Pleistocene carbonate slopes (e.g., Kier and Pilkey 1971), causing alternating Mg-rich and Mg-poor layers can also be invoked as a cause of cyclicity, but the close cluster of Sr values from both dolomite and limestone interbeds does not support this alternative.

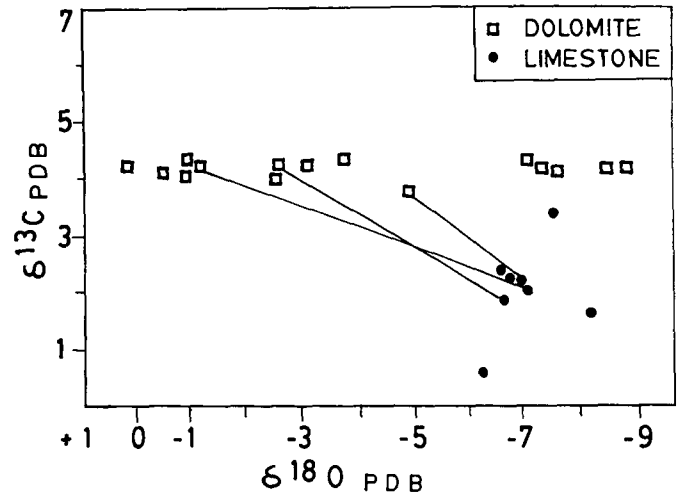


FIG. 14.—Stable-isotope plots for dolomite and limestone. Samples from adjacent beds of a couplet with both dolomite and limestone analyses are connected by tie lines.

Early diagenetic dolomitization in normal marine pore water proposed in the model (Fig. 15) warrants a mass-balance consideration. On average, limestone beds are twice as thick as dolomitic limestone beds; a 2 cm dolomitic bed overlies a 4 cm limestone bed, thereby forming a 6 cm couplet. The 2 cm dolomitic interval, which is one third of the total volume of the couplet, contains 40–45% dolomite and the rest calcite, whereas the 4 cm limestone interval at the base of the couplet, two thirds of the total volume of the couplet, contains negligible dolomite. In terms of total volume of the couplet, dolomite forms only about 13–15% of the constituents. In the dolomitic bed, about 45% nonstoichiometric dolomite ($Ca_{0.56-0.54}Mg_{0.44-0.46}CO_3$) and 55% calcite ($Ca_{0.99}Mg_{0.01}CO_3$) sum to about 21–22 mole % $MgCO_3$. The proposed model considers derivation of the total Mg from within the precursor 6 cm Mg-calcite interval. Considering that Mg-calcite may retain about 2 mole % $MgCO_3$ (Scoffin 1987, p. 111; Satterley et al. 1994) as a stable phase during shallow burial, an original 9 mole % $MgCO_3$ in the precursor phase would be sufficient for partial dolomitization. The following mass balance can be proposed in favor of this hypothesis of partial dolomitization:

$$Ca_{.91}Mg_{.09}CO_3 = .85\ Ca_{.98}Mg_{.02}CO_3 + .15\ Ca_{.56-.54}Mg_{.44-.46}CO_3.$$

Incomplete transformation of nonstoichiometric to stoichiometric dolomite is further likely to support a low Mg/Ca ratio of the solution, which in turn is consistent with an indigenous source of Mg, as proposed in this model.

## CONCLUSION

Bedding-parallel rhythmic dolomite-limestone alternation in the deep-marine Proterozoic Chanda Limestone is formed by penecontemporaneous dolomitization. Stratigraphic, petrographic, and geochemical data collectively suggest that dolomitization occurred in the marine pore water during shallow burial diagenesis. Gradual decline in dolomite content from the base to the top of a dolomitic bed, and rhythmic alternation of dolomite and dolomitic limestone, are attributed to diagenetic alteration of precursor high-magnesium calcite. Upward escape of Mg-rich pore fluid leads to periodic supersaturation with respect to dolomite.

## ACKNOWLEDGMENTS

Isotope analyses were carried out at the University of Texas at Austin. We gratefully acknowledge Dr. L.S. Land and Dr. G. Gao for the isotope analysis. We

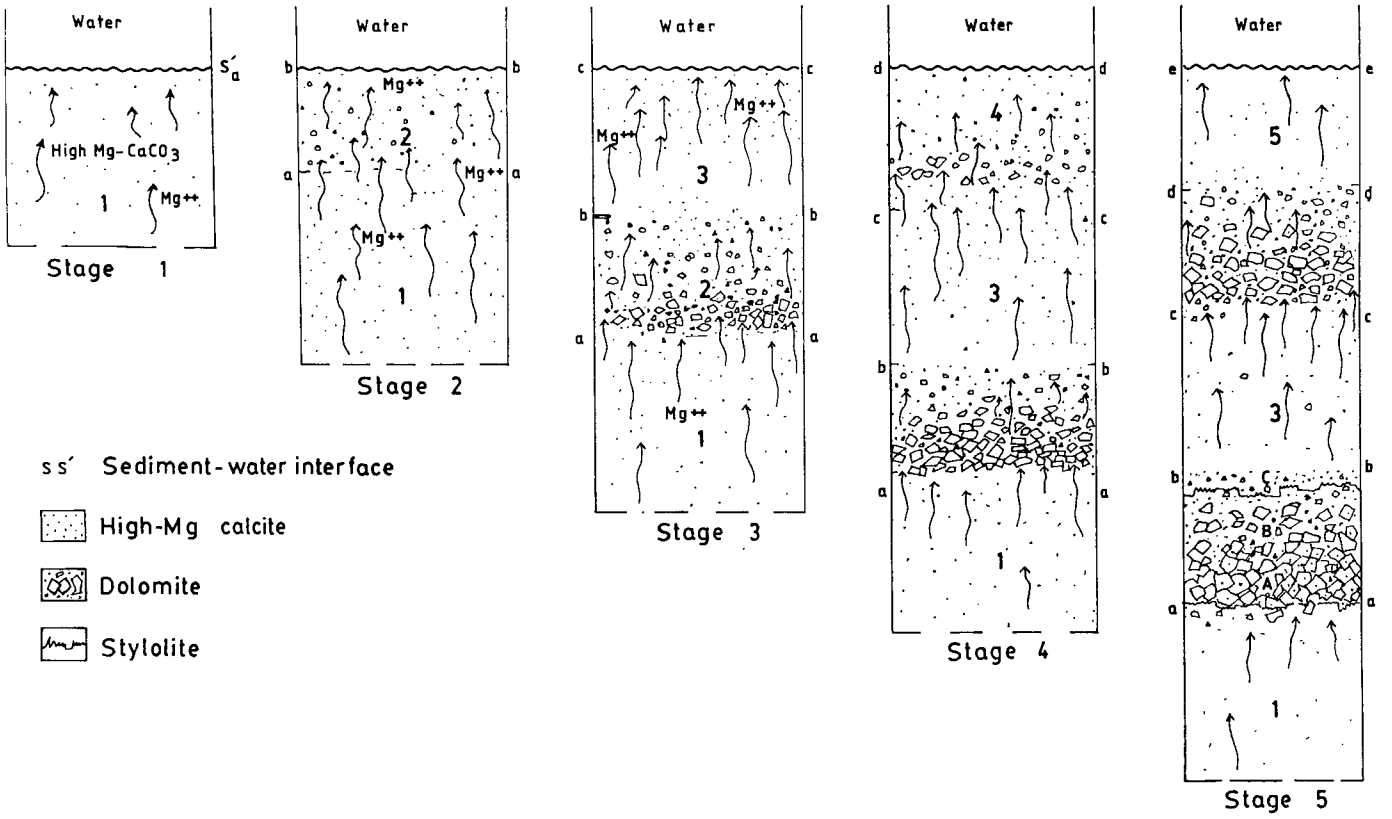


FIG. 15.—Schematic model of development of rhythmicity in dolomite-bearing sequence. Stage 1: Incongruent dissolution of high-Mg calcite under shallow burial, near sediment-water interface; migration of $Mg^{2+}$ to overlying sediments. Stage 2: Rapid burial in Layer 2, enrichment of Layer 2 in Mg, and nucleation of dolomite. Stage 3: Progressive dolomitization of Layer 2 above aa and deposition of Layer 3. Stage 4: Sedimentation above (cc) and deposition of Layer 4. With continued burial development of different fabric in layer 2, $Mg^{2+}$ released from Layer 1 is used up in Layer 2; Layer 3 acted as the source of Mg for layer 4. Stage 5: Complete dolomitization in Layer 2 with development of Types A, B, and C fabrics. Pressure-solution operates near the limestone-dolomite boundaries. Progressive dolomitization in Layer 4. Repetition of the same process in Layer 5.

acknowledge valuable suggestions from Dr. L.S. Land. We are grateful to Dr. Somnath Dasgupta for providing the trace-element analyses. We are grateful to Drs. M. Coniglio, A. Saller, and G.R. Dix for critical review of the manuscript. Logistics for the field work were provided by the Indian Statistical Institute, Calcutta. Financial support for field and laboratory work was provided by the University Grants Commission, India, to JM. We acknowledge the field assistance of S.N. Das. Drafting was done by A.K. Das. This work is a part of the Ph.D. dissertation of JM.

## REFERENCES

ANDERSON, T.F., AND ARTHUR, M.A., 1983, Stable isotopes of oxygen and carbon and their application to sedimentological and paleoenvironmental problems, *in* Arthur, M.A., Anderson, T.F., Kaplan, I.R., Veizer, J., and Land, L.S., eds., Stable Isotopes in Sedimentary Geology: Society of Economic Paleontologists and Mineralogists Short Course 10, p. 1–1–1–151.

BADIOZAMANI, K., 1973, The Dorag dolomitization model—application on the Middle Ordovician of Wisconsin: Journal of Sedimentary Petrology, v. 43, p. 965–984.

BENCE, A., AND ALBEE, A., 1968, Empirical correlation factors for the electron microanalysis of silicates and oxides: Journal of Geology, v. 76, p. 382–403.

BOSE, P.K., AND SARKAR, S., 1991, Basinal autoclastic mass-flow regime in the Precambrian Chanda Limestone Formation, Adilabad, India: Sedimentary Geology, v. 73, p. 299–315.

CANDER, H.S., KAUFMAN, J., DANIELS, L.D., AND MEYERS, W.J., 1988, Regional dolomitization of shelf carbonates in the Burlington-Keokuk Formation (Mississippian), Illinois and Missouri: constraints from cathodoluminiscent zonal stratigraphy, *in* Shukla, V.J., and Baker, P.A., eds., Sedimentology and Geochemistry of Dolostones: SEPM Special Publication 43, p. 129–144.

CHAUDHURI, A.K., DASGUPTA, S., BANDOPADHYAY, G., SARKAR, S., BANDOPADHYAY, P.C., AND GOPALAN, A.K., 1989, Stratigraphy of the Penganga Group around Adilabad, Andhra Pradesh: Geological Society of India Journal, v. 34, p. 291–301.

CHAUDHURI, A.K., AND CHANDA, S.K., 1991, The Proterozoic Basin of the Pranhita-Godavari Valley: An overview, *in* Tandon, S.K., Pant, C.C., and Casshyap, S.M., eds., Sedimentary Basins of India: Nainital, Gyanodaya Prakashan, 283 p.

CHOQUETTE, P.W., AND JAMES, N.P., 1990, Limestones—The burial diagenetic environment, *in* McIlreath, I.A., and Morrow, D.W., eds., Diagenesis: Geoscience Canada, Reprint Series no. 4, p. 75–111.

CONIGLIO, M., AND JAMES, N.P., 1988, Dolomitization of deep-water sediments, Cow Head Group (Cambro-Ordovician), Western Newfoundland: Journal of sedimentary Petrology, v. 58, p. 1032–1045.

CONIGLIO, M., AND JONES, A.E.W., 1992, Diagenesis of Ordovician carbonates from North-east Michigan Basin, Manitoulin Island, Ontario: evidence from petrography, stable isotopes and fluid inclusions: Sedimentology, v. 39, p. 813–836.

DEAN, W.E., GARDNER, J.V., JANSA, L.F., CEPEK, P., AND SEIBOLD, E., 1977, Cyclic sedimentation along the continental margin of Northwest Africa, *in* Lancelot, Y., Seibold, E., et al., Initial Reports of the Deep Sea Drilling Project, v. 41: Washington, D.C., United States Government Printing Office, p. 965–989.

DIX, G.R., 1993, Patterns of burial and tectonically controlled dolomitization in an Upper Devonian, fringing-reef complex: Leduc Formation, Peace River Arch Area, Alberta Canada: Journal of Sedimentary Petrology, v. 63, p. 628–640.

EDER, W., 1982, Diagenetic redistribution of carbonate, a process forming limestone-marl alternation (Devonian and Carboniferous) Rheinisches Schiefergebirge, West Germany, *in* Einsele, G., and Seilacher, G., eds., Cyclic and Event Stratification: Berlin, Springer-Verlag, p.98–112.

EINSELE, G., 1982, Limestone-marl cycles (periodites): diagnosis, significance, cause and review, *in* Einsele, G., and Seilacher, G., eds., Cyclic and Event Stratification: Berlin, Springer-Verlag, p. 8–54.

FAIRCHILD, I.J., AND SPIRO, B., 1987, Petrological and isotopic implications of some contrasting Late Precambrian carbonates, NE Spitsbergen: Sedimentology, v. 34, p. 973–989.

FOLK, R.L., AND LAND, L.S., 1975, Mg/Ca-ratio and salinity: two controls over crystallization of dolomite: American Association of Petroleum Geologists Bulletin, v. 59, p. 60–68.

FRIEDMAN, G.M., 1959, Identification of carbonate minerals by staining methods: Journal of Sedimentary Petrology, v. 29, p. 87–97.

GAO, G., AND LAND, L.S., 1991, Early modification of Cool Creek dolomite, Middle Arbuckle Group, Slick Hills, southwest Oklahoma, USA: Origin and modification: Journal of Sedimentary Petrology, v. 61, p. 161–173.

GAO, G., LAND, L.S., AND FOLK, R.L., 1992, Meteoric modification of early dolomite and late dolomitization by basinal fluids, Upper Arbuckle Group, Slick Hills, southwestern Oklahoma: American Association of Petroleum Geologists Bulletin, v. 76, p. 1649–1664.

GREGG, J.M., 1988, Origin of dolomites in the offshore facies of the Bonneterre Formation (Cambrian), southeastern Missouri, *in* Shukla, V.J., and Baker, P.A., eds., Sedimentology and Geochemistry of Dolostones: SEPM Special Publication 43, p. 67–83.

GROTZINGER, J.P., 1989, Facies evolution of Precambrian carbonate depositional systems: emergence of the modern carbonate archetype, *in* Crevello, P.D., Wilson, J.L., and Sarg, F.J., eds., Controls on Carbonate Platform and Basin Development: SEPM Special Publication 44, p. 79–106.

HARDIE, L.A., 1987, Dolomitization: A critical view of some current views: Journal of Sedimentary Petrology, v. 57, p. 166–183.

HUDSON, J.D., 1977, Stable isotopes and limestone lithification: Geological Society of London Journal, v. 133, p. 637–660.

JAMES, N.P., AND CHOQUETTE, P.W., 1984, Diagenesis 9: Limestones—The meteoric diagenetic environment: Geoscience Canada, v. 11, p. 161–194.

JENKYNS, H.C., 1974, Origin of red nodular limestones (Ammonitico Rosso, Knollenkalke) in the Mediterranean Jurassic: A diagenetic model, *in* Hsü, K.J., and Jenkyns, H.C., eds., Pelagic Sediments: On Land and Under the Sea: International Association of Sedimentologists Special Publication 1, p. 249–271.

KIER, J.S., AND PILKEY, O.H., 1971, The influence of sea level changes on sediment carbonate mineralogy, Tongue of the Ocean, Bahamas: Marine Geology, v. 11, p. 189–200.

LAND, L.S., 1980, The isotopic and trace element geochemistry of dolomites: The state of the art, *in* Zenger, D.H., Dunham, J.B., and Ethington, R.L., eds., Concepts and Models of Dolomitization: Society of Economic Paleontologists and Mineralogists Special Publication 28, p. 87–110.

LAND, L.S., 1985, The origin of massive dolomite: Journal of Geological Education, v. 33, p. 112–125.

LUMSDEN, D.S., 1985, Secular variations in the dolomite abundance in deep marine sediments: Geology, v. 13, p. 766–769.

LUMSDEN, D.N., 1988, Characteristics of deep marine dolomite: Journal of Sedimentary Petrology, v. 58, p. 1023–1031.

LUMSDEN, D.N., AND CHIMAHUSKY, J.S., 1980, Relationship between dolomite nonstoichiometry and carbonate facies parameters, *in* Zenger, D.H., Dunham, J.B., and Ethington, R.L., eds., Concepts and Models of Dolomitization: Society of Economic Paleontologists and Mineralogists Special Publication 28, p. 123–127.

MACHEL, H.G., AND MOUNTJOY, E.W., 1986, Chemistry and environments of dolomitization—A reappraisal: Earth-Science Reviews, v. 23, p. 175–222.

MITCHELL, J.T., LAND, L.S., AND MISER, D.E., 1987, Modern marine dolomite cement in a north Jamaican fringing reef: Geology, v. 15, p. 557–560.

MIGASZEWSKY, Z., 1991, Devonian dolomites from Holy Cross mountains, Poland: a new concept of the origin of massive dolomites based on petrographic and isotopic evidence: Journal of Geology, v. 99, p. 173–190.

MOUNTJOY, E.W., AND HALIM-DIHRAJDA, M.K., 1991, Multiple phase fracture and fault-controlled burial dolomitization, Upper Devonian, Wabamun Group: Journal of Sedimentary Petrology, v. 61, p. 590–612.

MULLINS, H.T., DIX, G.R., GARDULSKI, A.F., AND LAND, L.S., 1988, Neogene deep-water dolomite from the Florida-Bahamas Platform, *in* Shukla, V.J., and Baker, P.A., eds., Sedimentology and Geochemistry of Dolostones: SEPM Special Publication 43, p. 235–243.

MULLINS, H.T., WISE, S.W., LAND, L.S., SIEGEL, D.L., MASTERS, P.M., HINCHEY, E.J., AND PRICE, K.R., 1985, Authigenic dolomite in Bahamian periplatform slope sediment: Geology, v. 13, p. 292–295.

PERRY, E.C., AND AHMAD, S.N., 1983, Oxygen isotope geochemistry of Proterozoic chemical sediments: Geological Society of America Memoir 161, p. 253–263.

SALLER, A.H., 1984, Petrologic and geochemical constraints on the origin of sub-surface dolomite, Enewetak Atoll: An example of dolomitization by normal sea water: Geology, v. 12, p. 217–220.

SARKAR, S., 1991, Off-platform dolomitization in Proterozoic Chanda Limestone Formation, Adilabad, Andhra Pradesh: Indian Journal of Earth Science, v. 18, p. 209–218.

SARKAR, S., BOSE, P.K., AND FRIEDMAN, G.M., 1993, Ordered, stoichiometric dolomitization: A result of prolonged exposure to warm sea water: Proterozoic Chanda Limestone, Adilabad, India: Carbonates and Evaporites, v. 8, p. 109–117.

SATTERLEY, A.K., MARSHALL, J.D., AND FAIRCHILD, I.J., 1994, Diagenesis of an Upper Triassic reef complex, Wild Kirch, Northern calcareous Alps, Austria: Sedimentology, v. 41, p. 935–950.

SCHWAB, F.L., 1978, Secular trends in composition of sedimentary rock assemblages—Archean through Phanerozoic time: Geology, v. 6, p. 532–536.

SCOFFIN, T.P., 1987, An Introduction to Carbonate Sediments and Rocks: Glasgow, Blackie, 274 p.

SIBLEY, D.F., 1982, Origin of common dolomite fabrics: clues from the Pliocene: Journal of Sedimentary Petrology, v. 52, p. 1087–1100.

SIBLEY, D.F., 1990, Unstable to stable transformation during dolomitization: Journal of Geology, v. 98, p. 739–748.

SIBLEY, D.F., AND GREGG, J.M., 1987, Classification of dolomite textures: Journal of Sedimentary Petrology, v. 57, p. 967–975.

SMITH, T.M., AND DOROBEK, S.L., 1993, Alteration of early formed dolomite during shallow to deep burial: Mississippian Mission Canyon Formation, Central to South Montana: Geological Society of America Bulletin, v. 105, p. 1389–1399.

SPERBER, C.M., WILKINSON, B.H., AND PEACOR, D.R., 1984, Rock composition, dolomite stoichiometry and rock/water reactions in dolomitic carbonate rocks: Journal of Geology, v. 92, p. 609–622.

TUCKER, M.E., 1982, Precambrian dolomites: petrographic and isotopic evidence that they differ from Phanerozoic dolomites: Geology, v. 10, p. 7–12.

TUCKER, M.E., 1983, Diagenesis, geochemistry and origin of Precambrian dolomite. The Beck Spring dolomite of Eastern California: Journal of Sedimentary Petrology, v. 53, p. 1097–1120.

TUCKER, M.E., 1984, Calcite, aragonite and mixed calcitic aragonite ooids from the mid-Proterozoic Belt Supergroup, Montana: Sedimentology, v. 31, p. 627–644.

TUCKER, M.E., 1992, The Precambrian–Cambrian boundary: sea-water chemistry, ocean circulation and nutrient supply in Metazoan evolution, extinction and biomineralisation: Geological Society of London Journal, v. 149, p. 655–668.

TUCKER, M.E., AND WRIGHT, V.P., 1990, Carbonate Sedimentology: Oxford, Blackwell Scientific Publications, 482 p.

VEIZER, J., LEMIEUX, J., JONES, B., GIBLING, M.R., AND SAVELLE, J., 1978, Paleosalinity and dolomitization of a Lower Paleozoic carbonate sequence, Somerset and Prince of Wales Islands, Arctic Canada: Canadian Journal of Earth Sciences, v. 15, p. 1448–1461.

WANLESS, H.R., 1979, Limestone response to stress: Pressure-solution and dolomitization: Journal of Sedimentary Petrology, v. 49, p. 253–276.

ZENGER, D.H., DUNHAM, J.B., AND ETHINGTON, R.L., EDS., 1980, Concepts and Models of Dolomitization: Society of Economic Paleontologists and Mineralogists Special Publication 28, 320 p.

Received 15 March 1993; accepted 3 August 1994.